THE ASTROPHYSICAL JOURNAL, 273:L75–L79, 1983 October 15

DISTANCE TO THE 1.5 MILLISECOND PULSAR AND OTHER 4C 21.53 OBJECTS

CARL HEILES, SHRINIVAS R. KULKARNI, MARY A. STEVENS, AND D. C. BACKER
Radio Astronomy Laboratory, University of California, Berkeley
M. M. DAVIS
Arecibo Observatory
AND
W. M. GOSS
Kapteyn Astronomical Institute, University of Groningen, The Netherlands
Received 1983 April 19; accepted 1983 June 7

ABSTRACT

The distance to the 1.5 millisecond pulsar is estimated as 5 kpc based on neutral hydrogen absorption measurements. Two nearby sources, which along with the pulsar constitute the 4C 21.53 complex of radio sources, are shown to be more distant than the pulsar. In particular, 4C 21.53W, the H II region adjacent to the pulsar is about 10.7 kpc distant and clearly unrelated. The pulsar H I absorption measurement required development of a new observing technique which is described in detail.

Subject heading: pulsars

I. INTRODUCTION

The recently discovered millisecond pulsar 1937+21 (Backer *et al.* 1982, hereafter Paper I) lies in the "4C 21.53 complex." This complex consists of three components: (*a*) 4C 21.53E, a steep-spectrum ($\alpha \sim -1.2$), compact double source east of the pulsar presumably of extragalactic origin; (*b*) 4C 21.53W, a flat-spectrum ($\alpha \sim -0.1$), extended ($\sim 1'$) object to the west; and (*c*) a steep-spectrum ($\alpha \sim -2.5$), compact object which is the pulsar itself. Soon after the discovery of the millisecond pulsar, the extended object was found to be an H II region, and the question arose whether the H II region and the pulsar were associated or if their relation were a mere coincidence in the sky. In fact it was this apparent coincidence of a compact, steep-spectrum object with a flat-spectrum, extended object that provided the stimulus for the pulsar search, since the only other such combination known in the galaxy is the Crab nebula–Crab pulsar combination. In Paper I, two facts led us to suggest that the pulsar and the H II region were related: (*a*) the two objects are in the same area of sky in a region of relatively low radio confusion, and (*b*) the brightest part of the H II region and the pulsar are displaced to opposite sides of the nearly circular, low-level contours of the H II region. Clearly, however, a determination of the distances to the H II region and to the pulsar is required to settle the question.

The nominal distance to the pulsar is about 2.4 kpc, based on its dispersion measure of 71.2 pc cm^{-3} and an assumed electron density of 0.03 cm^{-3}. The nominal distance to the H II region (located at $l = 57^\circ.5$, $b = -0^\circ.3$) is either very small ("the near distance") or about 10.7 kpc ("the far distance"), based on the +2 km s^{-1} velocity of the H166α recombination line reported in Paper I. In this and subsequent calculations, we have used $R_0 = 10$ kpc, $\Theta_0 = 250$ km s^{-1}, and the Schmidt rotation curve for $R < R_0$. If these nominal distances are correct, then the two objects are not associated. The observations reported herein were made to confirm this tentative conclusion.

II. OBSERVATIONS

a) Aperture Synthesis Observations of 4C 21.53W and 4C 21.53E

We obtained an H I absorption spectrum toward 4C 21.53W with the Very Large Array (VLA), and H I absorption spectra toward 4C 21.53E and 4C 21.53W with the Westerbork synthesis radio telescope (WSRT). Eleven VLA antennas were used in the D configuration for an observation lasting 10 hours. We used 128 spectral channels separated by 6.1 kHz and Hanning-smoothed to 12.2 kHz resolution, or 2.6 km s^{-1}. The result, shown in Figure 1*c*, was obtained by a vector average of all visibility data whose projected baseline lengths were longer than 300 m in order to reduce the contribution from the structure in H I emission. The WSRT observations were done with 63 spectral channels separated by 9.77 kHz, or 2.1 km s^{-1}, with a total of 5 hours of integration. The data were analyzed by standard methods. The 72 m and 144 m baselines were

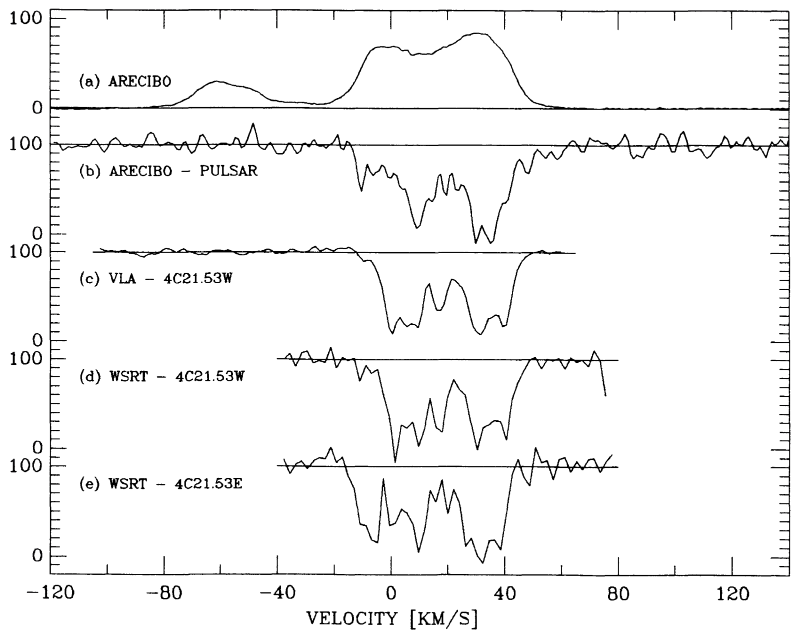

FIG. 1.—Neutral hydrogen emission and absorption spectra for 4C 21.53. The emission and absorption spectra toward the pulsar from Arecibo are presented in (*a*) and (*b*) respectively. The emission spectrum scale has units of degrees K and the absorption spectrum scale, here and below, has units of the fraction of continuum source intensity. The absorption spectra for the H II region, 4C 21.53W, are given in (*c*) and (*d*) based on synthesis observations with the VLA and WSRT respectively. The absorption spectrum for the extragalactic source 4C 21.53E from the WSRT is shown in (*e*).

excluded for reasons mentioned above. The WSRT absorption spectra for 4C 21.53W and 4C 21.53E are shown in Figures 1*d* and 1*e* respectively.

b) Arecibo Observations of the Pulsar

We devised a "phase-switching" method to obtain the H I-absorption spectrum since the high pulsing rate of the pulsar prevented the use of the standard techniques used in the past (see, for example, Weisberg 1978). This new method is described in some detail since it is very well suited to absorption spectroscopy of short-period pulsars. The correlator is used to form a continuous cross-correlation between one version of the input signal and a second version which is multiplied by $+1$ over the first half of the period and by -1 over the next half. The result is thus the difference between the pulse being "on" and "off." We actually switched the phase at twice the pulsar frequency, using both the main pulse and the half-period away interpulse as the "on" portion. This technique was straightforward to implement but is not the optimum with respect to the signal-to-noise ratio since the pulse widths are smaller than one-quarter of the pulse period.

In our phase-switching method, the incoming IF signal is split into two portions. Phase-switching is implemented by modulating the phase of one of the IF local oscillators (LO) by a phase-switching function which is 0° for the first half of the switching period and 180° for the next half. The arrival time of the pulse (i.e., the main pulse or the interpulse) at the band center frequency is adjusted to be in the center of the phase-switching square wave. The resulting cross-correlation function (CCF), $\Delta\rho(\tau)$, can be shown to be

$$\Delta\rho(\tau) = \Delta\rho_c(\tau)\cos(\Theta) + \Delta\rho_s(\tau)\sin(\Theta), \quad (1)$$

where

$$\Delta\rho_c + i\Delta\rho_s = \int S(\omega)\exp(i\omega\tau)\,d\omega. \quad (2)$$

$S(\omega)$ is the (complex) cross-power spectrum at the input to the correlator and ω refers to video frequencies. Here Θ is the phase shift of one IF signal with respect to the other and arises from the different electronic paths of the two IF signals. Since Θ is in general nonzero, one has to measure $\Delta\rho(\tau)$ for both positive and negative lags.

$S(\omega)$ contains $p(\omega)$, the pulsar pulse in absorption, and two instrumental contributions. The instrumental contributions, which result from the departure of the phase-switching function (PSF) from the square-wave function are $h(\omega)$, the galactic H I in emission, and $t(\omega)$, the instrumental (viz. receiver and spillover) noise. All three (complex) cross-power spectra are the original (real) power spectra modified by the introduction of the

PSF. In addition, $p(\omega)$ reflects the modifications due to the pulsating nature of the pulsar signal. One can express $S(\omega)$ as

$$S(\omega) = p(\omega) + \varepsilon(\omega)[h(\omega) + t(\omega)] + O(\varepsilon^2). \quad (3)$$

The function $\varepsilon(\omega)$ is proportional to the error in the phase-switching angles and can be expressed as

$$\varepsilon(\omega) = \varepsilon_0 + \omega\tau_{\text{diff}}. \quad (4)$$

Here the term $\omega\tau_{\text{diff}}$ accounts for the fact that the path lengths suffered by the two inputs to the cross-correlator are not exactly the same.

We separated the pulsar absorption spectrum, $p(\omega)$, from the instrumental contributions by making a least squares fit on a channel by channel (j) basis to a three-parameter function,

$$S(j) = \frac{[a(j)T_{\text{sys}}(t) + b(j) + \tau'(j)\langle T_p(t)\rangle]}{T_0};$$

$$j = 1\text{–}252. \quad (5)$$

Here, T_{sys} represents the system temperature, which varies with time because of spillover; T_0 is the system temperature at the beginning of the observation, when the clipping level was set to the optimum value of 0.61 of the input rms voltage; $\langle T_p\rangle$ represents the incoming pulsar power averaged across the spectrum, which varies with time because of interstellar scintillation; $\tau'(j)$ is the (approximate) optical depth of the pulsar absorption spectrum; $b(j)$ is a constant instrumental spectrum; and $a(j)$ is a second component of the instrumental spectrum which is proportional to the system temperature. T_{sys} was measured by power counters in the correlator; $\langle T_p\rangle$ was estimated from the value of the zero lag channel of the CCF, $\Delta r(0)$. Kulkarni and Heiles (1980, hereafter KH) show that

$$[\langle T_p(t)\rangle + K]/T_0 = (2/c)\{\Delta r(0)/[dr(0)/dc]\}, \quad (6)$$

$$r(0) = (1/\pi)\int_0^{(\pi/2)-\Theta}\{\exp[-c^2/(1+\sin\phi)] + \exp[-c^2/(1-\sin\phi)]\}\,d\phi. \quad (7)$$

In equation (6), K is the integrated power from the instrumental terms in equation (3); c^2 is $0.61[T_0/T_{\text{sys}}(t)]$. Owing to absorption of H I, $\langle T_p\rangle$ is an underestimation of the antenna temperature in the continuum. Hence $\tau'(j)$ is an overestimation of the optical depth of the pulsar absorption line. The true optical depth spectrum is $\tau'(j)$ scaled by a factor derived from an estimate of the total absorption of the pulsar signal.

The pulsar absorption spectrum derived by the new phase-switching technique is shown in Figure 1*b*. The emission spectrum in the direction of the pulsar is shown in Figure 1*a*.

The attainable velocity resolution is limited to roughly the inverse of the pulse width. Let $s(\omega)$ be the absorption spectrum one would obtain if the pulsar were a steady source. The measured power spectrum is related to $s(\omega)$ by the relation

$$p(\omega) = \int s(\omega')w(\omega - \omega')\,d\omega', \quad (8)$$

where $w(\omega)$ is the Fourier transform of the following function,

$$W(\tau) = \int_0^T g(t)g(t-\tau)\exp[-i\phi(t)]\,dt; \quad (9)$$

here $\phi(t)$ is the phase-switching function; T is the pulse repetition period; and $g(t)$ is the pulsar pulse voltage envelope function. The pulse can be approximated by a Gaussian of FWHM of 50 μs (Ashworth, Lyne, and Smith 1983; Stinebring 1983), and hence $w(\omega)$ is a Gaussian with a width of 17.7 kHz. Thus the ultimate resolution at the 21 cm line is 3.7 km s^{-1}.

Interstellar dispersion leads to a second complication. For sufficiently large disperison measures, the pulse at some frequencies within the observing band will straddle the 0° and 180° phase transition of the PSF. This would result in loss of power in the cross-power spectrum at those frequencies. Fortunately for the case of PSR 1937 +21, this contingency did not arise. Nevertheless, even if this happy situation were not the case, we could still recover the cross-power spectrum by the use of a PSF which is shifted with respect to the square-wave PSF mentioned above by 90° of pulse phase. Alternatively one could overcome this problem by employing a PSF, $\phi(t) = \cos(2\pi t/T)$. In this case, the phase of the cross-power spectrum consists of an instrumental offset, a linear term from equation (4) and a quadratic term from dispersion. This particular phase-switching scheme resembles spectral line interferometry. Whereas, in interferometry, the phase relates to the source-baseline geometry, here the phase relates to the arrival phase of the pulse in the pulse window. As in spectral line interferometry, one need not measure the "sine" and "cosine" components separately, but instead need only measure the CCF for both negative and positive lags.

One final subtle point concerns the clipping corrections that one has to apply to the measured CCF. These have been extensively discussed by KH. To convert the measured CCF, $\Delta r(\tau)$, $\tau \neq 0$, to $\rho(\tau)$, the true CCF, the "lower inversion formula" of KH should be used. However, for $\tau = 0$, the applicable formula is the "upper inversion" approximation of KH, even though $|\Delta r(0)| \ll 1$ because $\Delta r(0)$ is really the difference between two CCFs, each of whose $r(0)$ is large (i.e., whose $\rho(0)$ is close to unity).

III. DISCUSSION

The emission and absorption spectra presented in Figure 1*a*, through 1*e* show that 4C 21.53E has more H I absorption than 4C 21.53W which in turn has more than the pulsar. This shows that all three objects are spatially distinct; the most distant is 4C 21.53E and the closest is the pulsar. The line of sight to the "4C 21.53 complex" passes through the inner galaxy (i.e., $R < R_0$). Consequently, H I gas at two different locations, with the same galactocentric radius, will appear at the same radial velocity. The maximum positive radial velocity, 40 km s^{-1}, will be from the H I gas at the tangent point, which is located 5.4 kpc away from us and at a galactocentric radius of 8.5 kpc. All the absorption spectra show absorption over nearly all positive velocities. Thus, none of the components of the "4C 21.53 complex" is nearer than about 5 kpc.

The recombination line velocity of +2 km s^{-1} reported in Paper I and the absorption spectrum presented in Figure 1*c* places the H II region on the solar circle at the far distance of 10.7 kpc. From the H I maps of Kulkarni, Blitz, and Heiles (1982), we see that, in fact, the H II region is located in a rather prominent H I concentration in the Perseus arm. The mass of the ionized gas in the 1′ H II region deduced from the radio free-free flux density of 1 Jy at 1400 MHz is about 230 $M_\odot$; the required ionizing flux is about 10^{49} Lyman-continuum photons per second which can be supplied by a single O7 star or 28 B0 stars. The free-free luminosity of this H II region is comparable to that of the Orion nebula. Thus it may be a site of active star formation. Such a coincidence of star-formation sites with prominent H I concentrations has been noted by Blitz, Fich, and Kulkarni (1983) in the second and third quadrants. These authors also find that such sites are invariably associated with molecular complexes. On this basis, we predict that one would be able to detect CO from 4C 21.53W.

The pulsar absorption spectrum (Fig. 1*b*) does not have as much absorption as the spectrum toward the H II region. In considering the pulsar absorption spectrum, we must keep in mind that the effective velocity resolution for this pulsar is poorer than all of the other absorption spectra in Figure 1. The instrumental Hanning-smoothed resolution for the pulsar absorption experiment was 9.8 kHz. However, due to the effects discussed in § III, the effective velocity resolution for the pulsar absorption spectrum is about 4.2 km s^{-1}. Between 0 and 10 km s^{-1}, the pulsar hardly shows any absorption at all, and the 16 km s^{-1} component visible in the H II region spectrum does not appear in the pulsar spectrum. Furthermore, on close inspection, one can see that the pulsar spectrum does not show as much absorption at 40 km s^{-1} as do those of 4C 21.53E and 4C 21.53W (Fig. 1*c*–1*e*). Since this feature is located at the tangent point, we conclude that the pulsar is in fact a little closer to us than the tangent point, 5 kpc. The pulsar, in addition, shows a narrow absorption feature at −10 km s^{-1}, which we believe to arise from a nearby small dust cloud. This feature is also seen in the spectrum of 4C 21.53W.

Our 5 kpc distance to the pulsar is in good agreement with the distance implied by the dispersion measure if we assume that the average electron density at $l = 60°$ is about half the normal value of 0.03 cm^{-3}. Indeed, the pulsar H I absorption data do support such a low value. In a recent study of H I absorption, Weisberg (1978) finds an average electron density of 0.015 cm^{-3} toward PSR 2016+28 ($l = 68\overset{\circ}{.}1$, $b = -4\overset{\circ}{.}0$) and PSR 2020+28 ($l = 68\overset{\circ}{.}9$, $b = -4\overset{\circ}{.}7$). Ables and Manchester (1976) have linked the apparently lower electron densities in the longitude range 60°–70° to the fact that these lines of sight traverse long paths through the interarm region. Our data confirm their claim.

This line of sight is unusual in that it has three objects within a few arc minutes of each other but placed at different distances. One could thus use these objects to study the correlation between the optical depth integral and distance, following Dickey *et al.* (1981). Unfortunately, calibration difficulties prevent comparison of optical depth integrals at a meaningful level.

The absorption spectrum of 4C 21.53E, shown in Figure 1*e*, resembles the spectrum of 4C 21.53W at all positive velocities. Hence, it must be at least as distant as the H II region. In addition, 4C 21.53E has considerable absorption at negative velocities from gas more distant than 11 kpc. We conclude that 4C 21.53E is beyond the H II region. Since 4C 21.53E is a $0\overset{''}{.}8$ double source (Paper I), it is almost certainly an ordinary, extragalactic, double-lobe radio source.

Optical pulses have now been detected from the pulsar by Manchester, Peterson, and Wallace (1983). Using their estimate of the apparent R-magnitude of about 24.5 mag and our estimate of A_v of about 9 mag based on the standard reddening parameters of 0.61 $E(B-V)$ kpc^{-1} and $R_v = 3$, we deduce the R absolute magnitude of the pulsar to be about 4.5 mag. Thus the optical luminosity of the pulsar is about 1 $L_\odot$, i.e., about 4×10^{33} ergs s^{-1}. In contrast to this luminosity, Becker and Helfand (1983) have an upper limit to the X-ray luminosity in the *Einstein* HRI energy range (0.1–3.4 kev) of 7×10^{31} ergs s^{-1} for an assumed distance of 2.5 kpc. With our estimate of the distance to the pulsar, this limit is raised to $3 \times 10^{32} \exp(-\tau)$ ergs s^{-1}, where $\tau = 5.2\,(E/\text{kev})^{-8/3}$. This new upper limit is consistent with Grindlay's (1983) claim of the detection of the pulsar in the *Einstein* data with a measured luminosity of about 10^{32} ergs s^{-1}. Thus the optical flux exceeds the X-ray flux by at least a factor of 10. The 20th magnitude star identified by Djorgovski (1982) has now been identified to be a K giant by Middleditch *et al.* (1983), surprisingly at about the same distance as the pulsar with a visual extinction of about 8–10 mag—in agreement with our rough estimate of extinction toward the pulsar.

The Crab and the Vela, the two fastest pulsars in our vicinity, are strong emitters of γ-rays. The total energy loss of PSR 1937+21, for a $\dot{P}$ of 10^{-19} s s^{-1}, is about 10^{36} ergs s^{-1}, comparable to Vela. If this pulsar has the same γ-ray conversion efficiency as Vela, then the γ-ray flux density of the more distant millisecond pulsar is smaller than that of Vela by a factor of 100 and consequently unobservable by *COS B*.

The pulsar is located 25 pc below the galactic plane. If its progenitor star was a member of the extreme Population I, then it probably has traversed no more than 145 pc in its lifetime. The kinematic age for the pulsar is 1.2×10^6 years if the pulsar has a transverse motion of 120 km s^{-1} (Backer, Kulkarni, and Taylor 1983). An upper limit to its age as a pulsar is given by the electromagnetic torque spin down time of $P/(2\dot{P}) \sim 2 \times 10^8$ years. The two age estimates can be made consistent by assuming either a lower transverse velocity and, or, an initial spin very close to the present value.

We would like to thank Don Campbell, Director of Arecibo Observatory, for allocating a generous amount of time for the Arecibo absorption project. The Very Large Array (VLA) is operated by the National Radio Astronomy Observatory under contract from the National Science Foundation. The Arecibo Observatory is operated by the National Astronomy and Ionospheric Center under contract from the National Science Foundation. The Westerbork Synthesis Radio Telescope is operated by the Netherlands Foundation for Radio Astronomy with the financial support of the Netherlands Organization for the Advancement of Pure Research (Z. W. O.). This research was supported in part by NSF grant AST 8212058.

REFERENCES

Ables, J. G., and Manchester, R. N. 1976, *Astr. Ap.*, **50**, 177.
Ashworth, M., Lyne, A. G., and Smith, F. G. 1983, *Nature*, **301**, 313.
Backer, D. C., Kulkarni, S. R., Heiles, C., Davis, M. M., and Goss, W. M. 1982, *Nature*, **300**, 615 (Paper I).
Backer, D. C., Kulkarni, S. R., and Taylor, J. H. 1983, *Nature*, **301**, 314.
Becker, R. H., and Helfand, D. J. 1983, *Nature*, **302**, 688.
Blitz, L., Fich, M., and Kulkarni, S. R. 1983, *Science*, in press.
Dickey, J. M., Weisberg, J. M., Rankin, J. M., and Boriakoff, V. 1981, *Astr. Ap.*, **101**, 332.
Djorgovski, S. 1982, *Nature*, **300**, 618.
Grindlay, J. 1983, private communication.
Kulkarni, S. R., Blitz, L., and Heiles, C. 1982, *Ap. J. (Letters)*, **259**, L63.
Kulkarni, S. R., and Heiles, C. 1980, *A.J.*, **85**, 1413 (KH).
Manchester, R. N., Peterson, A., and Wallace, P. T. 1983, *IAU Circ.*, No. 3795.
Middleditch, J., Cudaback, D., Pennypacker, C., Oliver, B., Rieke, G. H., Lebofosky, M. J., McGraw, J. T., and Dearborn, D. 1983, preprint.
Stinebring, D. 1983, *Nature*, **302**, 690.
Weisberg, J. M. 1978, Ph.D. thesis, University of Iowa.

D. C. Backer, C. Heiles, S. R. Kulkarni, and M. Stevens: Radio Astronomy Laboratory, University of California, Berkeley, CA 94720

M. M. Davis: Arecibo Observatory, P. O. Box 995, Arecibo, PR 00613

W. M. Goss: Kapteyn Astronomical Institute, Postbus 800, 9700 AV, Groningen, The Netherlands